

Cognitive Beamformer Chips with Smart-Antennas for 5G and Beyond: Holistic FDSOI Technology Solutions including ASIC Correlators

Sidina Wane¹, Pablo Corrales¹, Michael Haider¹, Johannes Russer¹, Quang-Hung Tran¹,

Riccardo Giacometti², Nicolas Gross³

¹ eV-Technologies,

² Keysight Technologies,

³ MVG - France

Abstract — ASIC-based stochastic analog correlators combined with cognitive co-array signal-processing for MIMO systems are proposed based on the concept of *Macro-Pixel Mosaic* partitioning. The ASIC-based analog correlators are co-integrated with cognitive RFIC beamformer chips and smart-antenna arrays including down-converters. Several solutions: 2x2 (16 antennas) and 4x4 (64 antennas) arrays of RFIC beamformer chips are designed, fabricated and experimentally characterized. Multi-scale and multi-level Field-Field correlation-based near-field and far-field solutions with and without down-conversion are demonstrated for coupled MIMO phased-array steered beams. Perspectives for holistic FDSOI technology solutions, including RF-ADCs and adaptive body-biasing systems, are drawn in the perspectives of hybrid mm-wave and optical technologies co-integration beyond 5G era.

Keywords — Mosaic Macro-Pixel, ASIC Analog-Correlators, Co-array signal processing, MIMO, FDSOI, RF-ADC, 5G.

I. INTRODUCTION

Stochastically sampled arrays have been proposed in various applications including radar, ultrasound imaging and geology. The driving motivations are generally based on economic reasons for benefiting from a large aperture with reduced number of channels. Randomly sampled arrays have generally been considered to address the objective of beampatterns with low main-lobe width and small sidelobes, or optimal possible sampling of a random field. The novelty of this contribution includes the following innovative approach:

- Proposal of cognitive co-array [1] signal-processing using the concept of Multi-scale Macro-Pixel introduced in [2].
- Use of ASIC-based Analog Correlators and broadband Delay-Lines [3] with beamformer chips.

RFIC beamformer chips represent key building blocks for emerging 5G MIMO and phased-array systems [4-8] envisioned to meet new requirements for higher data rates with increased bandwidth. The choice of the RFIC beamformer chip technology drives the achievable performance in terms of linearity, RF power levels, in-band and out-of-band emissions,

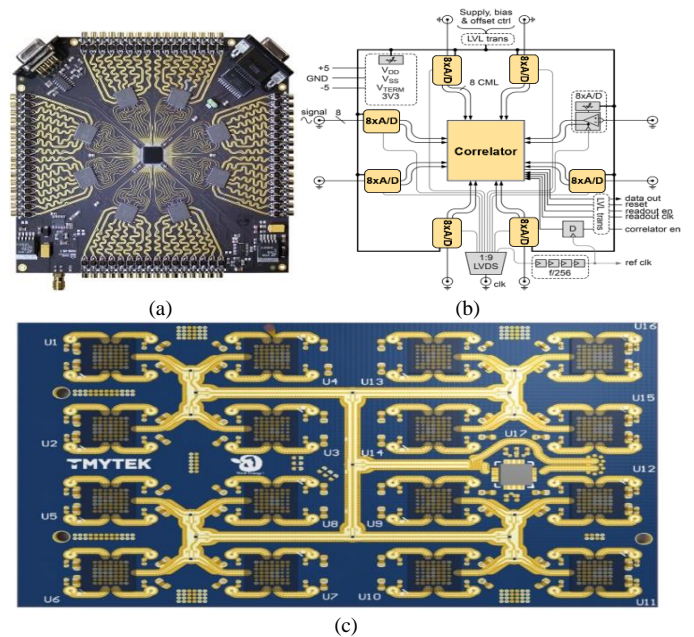


Fig. 1: (a), (b) Schematic and layout of commercial ASIC Analog Correlator Chip with 64-channel cross-correlator system. E. Ryman, et al., "1.6 GHz Low-Power Cross-Correlator Systems Enabling Geostationary Earth Orbit Aperture Synthesis", *IEEE Journal of Solid-State Circuits*, vol. 49, no. 11, Nov 2014. (c) eV-Technologies and TMYTEK 5G solution [4] integrating 4x4 beamformer RFICs with 8x8 smart-antennas and down-conversion.

sensitivity and energy-efficiency. Among the candidate technologies are GaAs, GaN, InP, high performance SiGe, and advanced CMOS options [9-11]. Comparative analysis of 45nm FDSOI CMOS and high performance SiGe BiCMOS technologies are presented in [12] for the design of a Ka band front-end-module (FEM) including a switch, low-noise amplifier (LNA), and power amplifier (PA). In general, GaAs, GaN and InP process options are challenging to integrate with logic although they can exhibit excellent [9] RF performances. Nevertheless, in sub-6GHz communication systems, mainstream FEM blocks tend to be implemented with chips from different processes that are integrated together with multi-chip module (MCM) or system-in-package (SiP) technologies

or on laminate/PCB board to optimize performance. PAs are preferably implemented with GaAs or SiGe, switches and LNAs are designed with SOI FET processes to get the advantage of low cost and improved performance, and digital control functionality using very cheap bulk CMOS. Beyond the intrinsic performance of RFIC beamformer chip technologies, system-level performance requires the proper integration with packaging and the application board while following holistic co-design strategies. The co-design of RFIC beamformer chips with smart-antennas appears as a strong enabler for the required tradeoffs between area constraints, power consumption, and broadband performance evaluated through over-the-air (OTA) near-field and far-field characterization accounting for stochastic environmental variations. Beyond the challenges of OTA tests, requirements of time-division-duplexing (TDD) for MIMO or massive-MIMO underscore the need for time-domain based broadband measurements and software based compensation in transmit and receive modes [13].

In this paper, 28GHz beamformer chips are combined with smart-antenna arrays and down-converters demonstrating MIMO and Massive-MIMO modules targeting the fifth-generation (5G) standard with Gb/s communication links based on 64 and 256 element phased arrays for coverage in the range of 100–300m radius with an equivalent isotropically radiated power (EIRP) of 55–65 dBm. Fig.1(c) represents the hardware implementation of the 5G MIMO module including down-conversion from RF to IF frequencies. The unitary RFIC beamformer chip is composed of 4 transmit/receive channels with a common RF terminal for input/output feed to power combiners/splitters. The unitary RFIC beamformer chip incorporates 4 PAs, 4 LNAs, 8 vector modulators (VMs), 1-to-8 splitter, SPI digital control bus, and 2 SPDT RF switches for TDD support. The following analyses were conducted for the co-design, co-simulation and experimental co-verification of the MIMO modules : (i) Global chip-package-PCB-antennas co-design and co-simulation using *Keysight* unified *SystemVue* platform linked to full-wave modeling capabilities (EMPro) and ADS thermal-electrical co-analysis. (ii) Frequency-domain far-field OTA evaluation using *MVG StarLab* and *TMYTEK BBOX* for MIMO and Massive-MIMO phased-array systems [14]. (iii) New time-domain near-field test solutions compliant with TDD [13] for 5G MIMO and massive-MIMO systems based on field-field correlations accounting for innovative co-array signal-processing [15] at IF and RF frequencies.

II. MAIN RESULTS AND EXPERIMENTAL VERIFICATION.

A. Experimental Setup of MIMO Phased-Array Systems for Broadband Characterization in Frequency and Time-Domains.

The following three measurement solutions were considered:

1. *TMYTEK* 5G Beamformer platform (Fig.2(a)) solutions
2. *Keysight* Time-Domain based measurement (Fig.2(b)).
3. *MVG StarLab* measurement platform (Fig.4(a)).

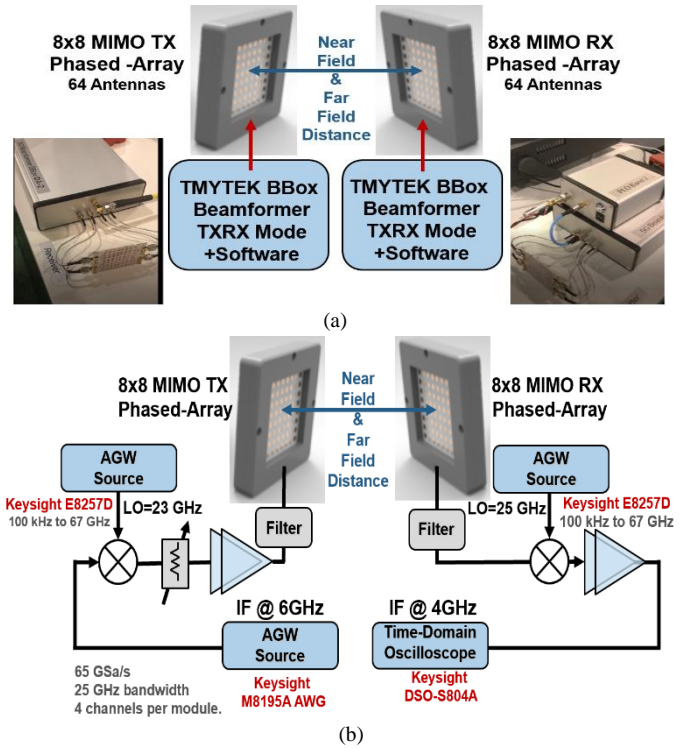


Fig. 2: (a) 28GHz phased-array based on TMYTEK BBOX beamformer system including signal processing/control. (b) Keysight measurement setup using high-resolution time-domain oscilloscopes with down-conversion.

Time-domain measurements at 28 GHz with bypassing of the mixer in Fig.2(b) have been conducted using a *Keysight DSA-X 96204Q* real-time oscilloscope. Sampling has been performed on a rectangular grid with 5 mm spacing at a distance of 8 cm from the DUT. The obtained phase distribution, here taken at the sampling limit, is shown in Fig. 3(a). The *StarLab* multi-probe array comprises a circular array of wide band (up to 50 GHz) probes that are evenly spaced along the circumference of a support structure.

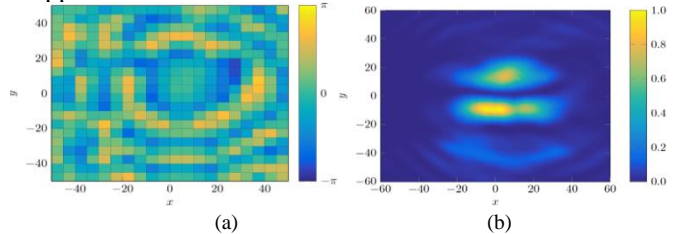


Fig. 3: (a) Spatial phase distribution of the radiated signal for a steering angle of 0°. (b) Normalized SED measured by near-field scanning at a steering angle of -25°.

The DUT is placed at the center of the support structure and measurements are made by electronically scanning the probe array in elevation and by rotating the DUT 180° in azimuth. By electronically scanning the multi-probe array the number of mechanical movements is minimized, thereby significantly reducing the time required to measurements. The system can measure antennas up to 45 cm. The radiation pattern for coupled phased-array beams can be seen in Fig. 4(b), for various steering angles coupled phased-array beams can be seen in Fig. 4(b), for various steering angles.

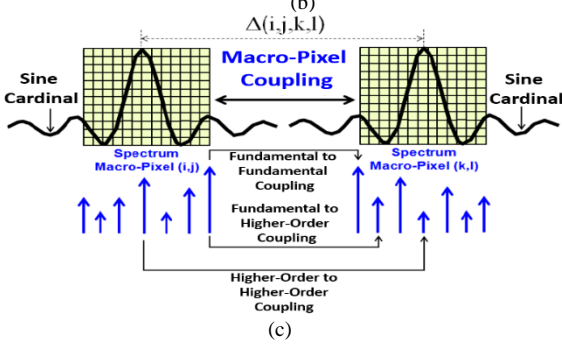
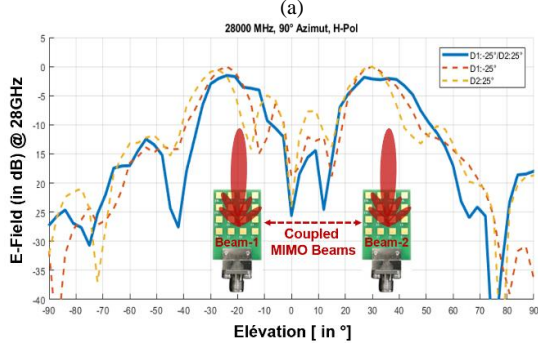
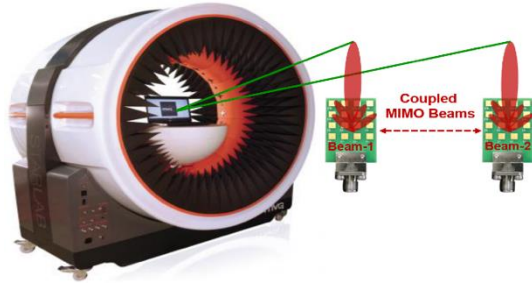


Fig. 4: *MVG StarLab* platform (a), Measured coupled beams with antenna array elements driven by RFIC beamformer chips operating at 28GHz (b), Macro-Pixel [2] *Mosaic* representation of coupled beams system (c).

The normalized spatial energy density (SED) distribution of the scanned tangential EM field for a steering angle of -25° is shown in Fig.3(b). Fig.3(b) shows the radiation scan for a steering angle of -25° , set at the phased-array, having two hot-spots visible in the plot. Here, the dominant hot-spot is the one located in the lower half of the plot, which corresponds to an angle of $\approx -25^\circ$. The near-field measurement setup consists of a probe positioning system with probing sensors, a signal generator, the antenna array under test, and a down-converter unit. We have performed measurements using a *Keysight DSA-X 96204Q* oscilloscope with a maximum sampling rate of 80 GS/s and with a *LeCroy SDA-813-Zi-A* oscilloscope with up to 40 GS/s. For numerical computation of far-field characteristics, the EM field has to be sampled with a spatial resolution which is governed by the wavelength and the proximity to the device under test. In close proximity to the device under test (DUT), this resolution can be substantially smaller than the wavelength. Fig.4(b) shows measured coupled beams with antenna array elements driven by RFIC beamformer chips operating at 28GHz using *MVG StarLab* 5G platform in Fig.4(a). ASIC-based stochastic analog correlators combined with cognitive co-Array signal-processing for MIMO systems are proposed based

on the concept of *Macro-Pixel Mosaic* [15] partitioning illustrated in Fig.4(c).

B. Macro-Pixel Concept for Cognitive Co-Array Signal-Processing of MIMO and Massive-MIMO Systems

Traditionally coupling is defined between sources through specified excitation modes. The concept of coupling between modes on different macro-pixels (composed of micro-pixels) can be understood as a generalization of the classical coupling between localized sources.

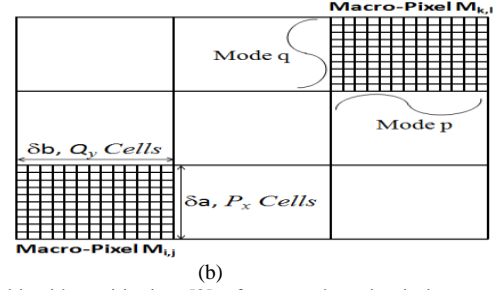
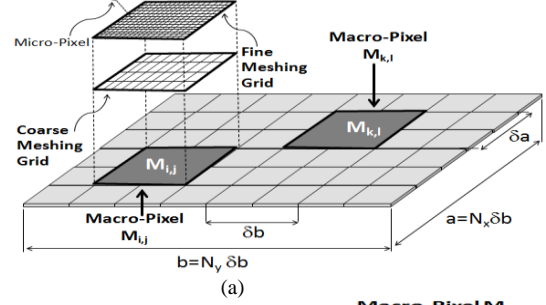


Fig.5: Multi-grid partitioning [2] of a complex circuit into macro-pixels, composed of micro-pixels (a). Green's functions coupling macro-pixel $M_{i,j}$ to macro-pixel $M_{k,l}$ with $P_x M_x = N_x$, $Q_y M_y = N_y$ (b).

In Fig.5, a multi-grid Green's function is considered to evaluate the correlations between macro-pixel of order (k, l) and macro-pixel of order (i, j) through fundamental and higher order modes versus a normalized distance $|i - k|$ or $|j - l|$. The partitioning domain is composed of 32×32 macro-pixels, each macro-pixel comprises 128 micro-pixels. The correlation resulting from the fundamental modes of the two macro-pixels is seen dominant by more than one decade in comparison with the higher order contributions. In Fig.5 the parameters p, q represent orders of local modes to the macro-pixel of order (k, l) and parameters p_0, q_0 designate orders of local modes on the macro-pixel of order (i, j) . p and p_0 refer to harmonics in the x direction; q and q_0 refer to harmonics in the y direction. It is observed from the curves of Fig.6 that, given a reference macro-pixel, the most dominant coupling arises with an area not exceeding an optimal number of neighboring macro-pixels: this optimal number is found to be around 7. This means that for distances between the macro-pixel source and observation sub-domain (another macro-pixel) greater than one-seventh of the wavelength only a reduced number of terms are sufficient to accurately extract the discrete Green's functions. In Fig.6 illustrative representation of macro-pixels interaction is shown where various couplings are highlighted: e.g., fundamental to fundamental, fundamental to higher order or higher order to higher order. The spectrum content represented in Fig.6 refers

to the modal basis functions local to each macro-pixel. Although the interactions between macro-pixels are derived in 2D representation, they can be easily extended to 3D description and can be also adapted to distributed couplings between spatially and/or spectrally coupled MIMO arrays.

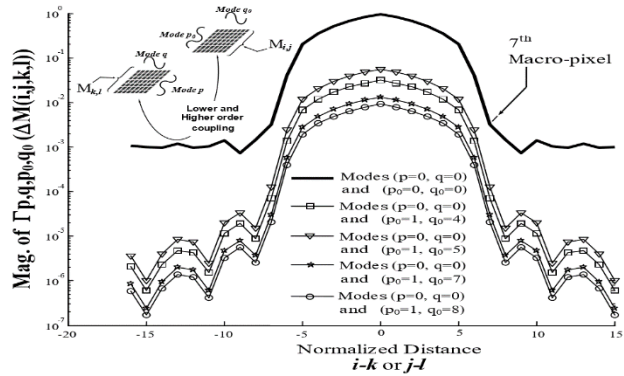


Fig.6: Coupling between macro-pixel of order (i, j) and macro-pixel of order (k, l) through fundamental mode on macro-pixel of order (i, j) and higher order modes on macro-pixel of order (k, l) versus a normalized distance $M(i, j) = |i - j|$, dominant coupling between fundamental modes [2].

The Cardinal-Sine function is well known in reference to Whittaker–Kotelnikov–Nyquist–Shannon Sampling Theorem. Taking benefit of the spatial and spectral properties of Cardinal Sine function, the interaction between macro-pixels can be formulated using Gabor Frames, following Dennis Gabor in his “Theory of Communication” on signal decomposition in terms of elementary signals established in 1946. Dennis Gabor in postulating that every square integrable function (in L^2 space) can be precisely represented as a series of translated and modulated copies of the Gaussian naturally bridges time-domain and frequency representations, since the Fourier transform of any Gaussian function is also a Gaussian function

III. CONCLUDING REMARKS

In this paper ASIC-based stochastic analog correlators combined with cognitive co-array signal-processing for MIMO systems are proposed based on the concept of *Macro-Pixel* [2] *Mosaic* partitioning. The concept of *Macro-Pixel Mosaic* partitioning opens new possibilities for combining multiple arrays into a full array state (*FAS*) to form one single beam, or for using them to form separate beams in the sub-array state (*SAS*). The resulting solutions can benefit from adaptive linearization techniques [16] accomplished based on sub-partitioned separate feedback (*FB*) paths, each of which considers the combined outputs of the multiple transmit units (e.g., *Power Amplifiers*) in one sub-array. Using multiport RF switches, the feedback paths are either considered individually, are all combined, or are partially combined (i.e. *grouped or clustered*) in accordance with how the sub-arrays may be merged to form beams. In the receive mode, multi-scale *Macro-Pixel Mosaic* [15] partitioning strategies are combined with Field-Field correlation-based near-field and far-field test solutions with and without down-conversion for MIMO or Massive-MIMO phased-array systems both in frequency and time domains. Perspectives for holistic [4] FDSOI [17] technology solutions, including RF-analog-to-digital

converters (RF-ADCs) and adaptive body-biasing [18] systems, are drawn in the perspectives of hybrid millimeter-wave [19] and optical technologies co-integration [20]. Such hybridization will foster a wide range of applications relative to mobile communications with smart devices and systems including machine learning and cognitive signal processing.

REFERENCES

- [1] J. F. Hopperstad and S. Holm, “The co-array of sparse arrays with minimum side-lobe level,” in Proceedings of IEEE NORISIG-98, June 1998, pp. 137–140.
- [2] S. Wane, D. Bajon, “Derivation of Multi-grid discrete and Analytic Green’s functions Free of Poles in terms of Transverse Waves,” IEEE MTT-S Int. Microwave Symp. Dig., San Francisco, USA June 2006.
- [3] S. Wane and D. Bajon, “Broadband Phase Control in Frequency and Time Domains: Design of True Delay-Lines for Noise-Decorrelation in Sensor-Arrays”, in Proc 2019 Texas Symposium on Wireless and Microwave Circuits and Systems (WMCS), Waco, TX.
- [4] S. Wane et al., “Millimeter-Wave Beamformer Chips with Smart-Antennas for 5G: Toward Holistic FDSOI Technology Solutions including RF-ADCs”, in Proc 2019 Texas Symposium on Wireless and Microwave Circuits and Systems (WMCS), Waco, TX.
- [5] J. P. Comeau et al., “A silicon-germanium receiver for X-band transmit/receive radar modules,” IEEE J. Solid-State Circuits, vol. 43, no. 9, pp. 1889–1896, Sep. 2008.
- [6] M. Parlak and J. F. Buckwalter, “A 2.9-dB noise figure, Q-band millimeter-wave CMOS SOI LNA,” in Proc. IEEE Custom Integr. Circuits Conf. (CICC), Sep. 2011, pp. 1–4.
- [7] Gabriel M. Rebeiz, et al., “”, MTT-S Int. Microwave Symp. Dig, 2017.
- [8] Kerim Kibaroglu et al., “A Scalable 64-Element 28 GHz Phased-Array Transceiver with 50 dBm EIRP and 8-12 Gbps 5G Link at 300 Meters Without Any Calibration,” MTT-S Int. Microwave Symp. Dig, 2018.
- [9] Bror Peterson., “5G Fixed Wireless Access Architectures and RF Front End Design,” in Microwave Journal 2018.
- [10] J. D. Dunworth et al., “A 28GHz Bulk-CMOS dual-polarization phased-array transceiver with 24 channels for 5G user and base station equipment,” 2018 IEEE International Solid - State Circuits Conference (ISSCC), San Francisco, pp. 70-72.
- [11] H. Al-Rubaye, G. M. Rebeiz, “W-Band Direct-Modulation >20-Gb/s Transmit and Receive Building Blocks in 32-nm SOI CMOS,” J. Solid-State Circuits 52(9): 2277-2291 (2017).
- [12] Chaojiang Li, et al., “Ka Band FEM Design Comparison with 45nm FDSOI CMOS and High Performance SiGe BiCMOS,” 2018 14th IEEE International Conference on Solid-State and Integrated Circuit Technology (ICSICT), pp. 1-4.
- [13] L. J. Foged, L. Scialacqua, F. Saccardi, N. Gross, A. Scannavini, “Over the Air Calibration of Massive MIMO TDD Arrays for 5G Applications,” 2017 IEEE International Symposium on Antennas and Propagation & USNC/URSI Meeting, pp. 1423 – 1424.
- [14] (2019). Microwave Vision Group website. [Online]. Available: <http://www.mvg-world.com/en>.
- [15] S. Wane, R. Patton, and N. Gross, “Unification of instrumentation and EDA tooling platforms for enabling smart chip-package-PCB-probe arrays co-design solutions using advanced RFIC technologies,” in IEEE Conf. on Antenna Measurements Applications, Sept 2018, pp. 1–4.
- [16] Raja N. Mir, “Linearization Approach for 5G Millimeter-Wave N-Array Beamforming Device”, in Proc 2019 Texas Symposium on Wireless and Microwave Circuits and Systems (WMCS).
- [17] J-P. Raskin, “SOI technology pushes the limits of CMOS for RF applications,” 2016 IEEE 16th Topical Meeting on Silicon Monolithic Integrated Circuits in RF Systems (SiRF), Austin, TX, 2016, pp. 17-20.
- [18] (2019) Dolphin Integration website. [Online]. Available: <https://www.dolphin-integration.com/>.
- [19] Asif, et al., “Frequency based design partitioning to achieve higher throughput in digital cross correlator for aperture synthesis passive MMW imager,” Sensors, Vol. 18, 1238, 2018.
- [20] S. Wane and N. Aflakian, “Photonics Chip-to-Chip Communication for Emerging Technologies: Requirements for Unified RF, mm-Waves and Optical Sensing”, in Proc 2019 Texas Symposium on Wireless and Microwave Circuits and Systems (WMCS).